AD-A091 971 ARETE ASSOCIATES ENCINO CA F/G 20/4
VISCOUS FLOW OVER ARBITRARY GEOMETRIES AT HIGH ANGLE OF ATTACK,(U)
JUN 79 W S HELLIWELL, R P DICKINSON F04701-78-C-0014
UNCLASSIFIED AR-79-052-TR NL

END
DATE FILMED
1-81
DTIC

ARETÉ ASSOCIATES

Santa Monica, CA

AR-79-052-TR

ABSTRACT

VISCOUS FLOW OVER ARBITRARY GEOMETRIES AT HIGH ANGLE OF ATTACK

By WILLIAM S. HELLIWELL
RICHARD P. DICKINSON
STEPHEN C. LUBARD +

JUNE 1979

+AIAA MEMBER

THIS WORK WAS SUPPORTED BY SAMSO
UNDER CONTRACT F04701-78-C-0014

P.O. BOX 350, ENCINO, CALIFORNIA 91316

ABSTRACT

1. INTRODUCTION

This paper presents a numerical method for obtaining the supersonic, laminar viscous flow about arbitrary geometries without compression surfaces at high angle of attack. In particular, results are presented for blunt biconic bodies with windward and leeward cuts. The basic approach used is to solve the steady three-dimensional "Parabolized Navier-Stokes Equations" (PNS), first derived for circular cones by Lubard and Helliwell [1,2] (see Figure 1). These equations have been used to predict the flowfield for a variety of different problems, including flow over sharp and blunt cones at angle of attack up to 40 deg. [3-5], flow over spinning cones at angle of attack [6], and flow over cones with mass transfer and temperature variation at the surface. In addition to these results which were confined to circular cones, some limited results have been obtained for biconic geometries [7], non-circular cones [8] and the NASA space shuttle [9].

For the three dimensional geometries of interest (e.g. Figure 1), we have developed a non-orthogonal curvilinear coordinate system that appears ideal for this problem. The governing equations are written in terms of the non-orthogonal coordinates and their metrics. The three velocity components are also defined in the non-orthogonal coordinate directions. This is different from writing the equations in an orthogonal coordinate system and explicitly performing a coordinate transformation.

Predictions using the new approach have been obtained for the body illustrated in Figure 1 at angles of attack up to 10° and a Mach number of 10. Surface pressure and heat transfer have been compared with wind tunnel data and show very good agreement.

2. COORDINATE SYSTEM AND EQUATIONS

The steady Navier-Stokes Equations are first written in general curvilinear coordinates, and then a particular coordinate system is chosen. One of the coordinates, ξ_1, is chosen in the general axial direction, another ξ_2, in a direction away from the body, and the third, ξ_3, around the body (Figure 2). It is assumed that coordinates with these characteristics and that the types of flows to be studied permit the approximations $\frac{\partial}{\partial \xi_1} << \frac{\partial}{\partial \xi_2}, \frac{\partial}{\partial \xi_3}$ in the viscous terms. The resulting system is called the "parolized Navier-Stokes" (PNS) equations.

In order to achieve validity of the PNS approximation, good finite difference approximations to the derivatives, and numerically accurate boundary conditions, it is desirable to have a coordinate system that has both body and shock surfaces as coordinate surfaces along with the ξ_2 coordinate orthogonal to these surfaces. To generate an orthogonal three-dimensional coordinate system with these properties would be a formidable task. If it is permitted that the ξ_1 and ξ_3 coordinates not necessarily be orthogonal, but are orthogonal to the ξ_2 coordinate, then a coordinate system with the above properties can be generated. In summary we construct the ξ_1, ξ_2, and ξ_3 coordinates so as to have the following properties:

1) The body is a coordinate surface ($\xi_2 = 0$).

2) The ξ_1 and ξ_3 coordinates are necessarily orthogonal only at the body.

3) The ξ_2 coordinate is orthogonal to ξ_1 and ξ_3.

4) The bow shock is a ξ_1, ξ_3 coordinate surface.

In order to generate these non-orthogonal coordinates, we start at the body and calculate out to the shock. The surface of the body is written in cylindrical coordinates as

$$r = r\ (z,\phi) \tag{1}$$

and $\underline{g}_i$ is defined to be a vector in the ξ_i direction with the coordinate metrics $g_{ij} \equiv \underline{g}_i \cdot \underline{g}_j$. The ξ_1 and ξ_3 coordinates on the body ($\xi_2 = 0$) are generated by using the method outlined by Blottner and Ellis in Reference (10).

The coordinates in the region from the body surface to the shock surface are obtained by taking the cross product, $\underline{g}_3 \times \underline{g}_1$. If $\underline{i}'$, $\underline{j}'$, $\underline{k}'$ are unit vectors in cylindrical coordinates, then the ξ_1 coordinate vectors are given by

$$\underline{g}_m = \frac{\partial z}{\partial \xi_m}\, \underline{i}' + \frac{\partial r}{\partial \xi_m}\, \underline{j}' + r\, \frac{\partial \phi}{\partial \xi_m}\, \underline{k}' \ , \quad m = 1,2,3. \tag{2}$$

Defining $\underline{n}$ as the cross product between $\underline{g}_3$ and $\underline{g}_1$, and using Equation (2), we obtain

$$\underline{n} = n_1\, \underline{i}' + n_2\, \underline{j}' + n_3\, \underline{k}' \tag{3}$$

where

$$\begin{aligned} n_1 &= r\left(\frac{\partial r}{\partial \xi_3}\frac{\partial \phi}{\partial \xi_1} - \frac{\partial \phi}{\partial \xi_3}\frac{\partial r}{\partial \xi_1}\right), \\ n_2 &= r\left(\frac{\partial \phi}{\partial \xi_3}\frac{\partial z}{\partial \xi_1} - \frac{\partial z}{\partial \xi_3}\frac{\partial \phi}{\partial \xi_1}\right), \\ n_3 &= \left(\frac{\partial z}{\partial \xi_3}\frac{\partial r}{\partial \xi_1} - \frac{\partial r}{\partial \xi_3}\frac{\partial z}{\partial \xi_1}\right). \end{aligned} \tag{4}$$

Now set $\dfrac{\underline{g}_2}{\sqrt{g_{22}}} = \dfrac{\underline{n}}{|\underline{n}|}$ and again use Equation (2) to obtain the

equations for $\frac{\partial z}{\partial \xi_2}$ $\frac{\partial r}{\partial \xi_2}$ and $\frac{\partial \phi}{\partial \xi_2}$. These equations can now be integrated *from* the body ($\xi_2 = 0$) to the shock in order to obtain z, r, and ϕ as functions of ξ_1, ξ_2, and ξ_3.

With the coordinates constructed in this manner, $\underline{g}_2$ is always orthogonal to $\underline{g}_1$ and $\underline{g}_3$ (i.e., $g_{23} = g_{21} = 0$), but g_1 is not necessarily orthogonal to $\underline{g}_3$. By setting $g_{22} = S(\xi_1,\xi_3)$, the shock distance, $\underline{g}_2$ will be orthogonal to the shock surface, and the shock will correspond to $\xi_2 = 1$. (Note that doing this makes the coordinate system a function of the solution since the shock distance is unknown.)

Figure 3 illustrates the resulting coordinates away from the body.

Once $z(\xi_1,\xi_2,\xi_3)$, $r(\xi_1,\xi_2,\xi_3)$ and (ξ_1,ξ_2,ξ_3) are known everywhere, the metrics g_{ij} can be obtained by differentiation, i.e.,

$$g_{ij} = \frac{\partial z}{\partial \xi i}\frac{\partial z}{\partial \xi j} + \frac{\partial r}{\partial \xi i}\frac{\partial r}{\partial \xi j} + r^2 \frac{\partial \phi}{\partial \xi i}\frac{\partial \phi}{\partial \xi j} \quad i,j = 1,2,3. \tag{5}$$

Knowing the metrics, the following important quantities used in the PNS equations can be computed. These are the determinant of the metric, g, which for our system is

$$g = g_{11}g_{22}g_{33} - g_{22}g_{13}^2 \tag{6}$$

and the Christoffel symbols of the second kind

$$\left\{ \begin{matrix} i \\ j\ k \end{matrix} \right\} = \sum_{m=1}^{3} g^{im} \frac{\partial g_{mk}}{\partial \xi_j} + \frac{\partial g_{mj}}{\partial \xi_k} - \frac{\partial g_{jk}}{\partial \xi_m} , \tag{7}$$

where the g^{ij} are defined by

$$\sum_{k=1}^{3} g^{ik} g_{kj} = \delta_j^i \quad . \tag{8}$$

The steady parabolized Navier-Stokes equations in non-dimensional form (References 1,2) can now be written. In order to derive the PNS equations, we assume for the viscous terms $\frac{\partial}{\partial \xi_1} << \frac{\partial}{\partial \xi_2}$ and $\frac{\partial}{\partial \xi_3}$ and that gradients of the coordinate metrics are of 0(1). No approximations are made to the inviscid terms. As an example, the ξ_1-momentum equation becomes

$$\frac{1}{g^{\frac{1}{2}}}\left[\frac{\partial}{\partial \xi_1}\left(\rho u^2 g^{\frac{1}{2}}\right) + \frac{\partial}{\partial \xi_2}\left(\rho uv g^{\frac{1}{2}}\right) + \frac{\partial}{\partial \xi_3}\left(\rho uw g^{\frac{1}{2}}\right)\right] + \rho\left[u^2 \begin{Bmatrix} 1 \\ 1 \quad 1 \end{Bmatrix}\right.$$

$$+ 2uv \begin{Bmatrix} 1 \\ 1 \quad 2 \end{Bmatrix} + 2uw \begin{Bmatrix} 1 \\ 1 \quad 3 \end{Bmatrix} + v^2 \begin{Bmatrix} 1 \\ 2 \quad 2 \end{Bmatrix} + 2vw \begin{Bmatrix} 1 \\ 2 \quad 3 \end{Bmatrix}$$

$$\left. + w^2 \begin{Bmatrix} 1 \\ 3 \quad 3 \end{Bmatrix}\right] + \frac{g_{22}}{g}\left[g_{33} \frac{\partial \rho}{\partial \xi_1} - g_{13} \frac{\partial \rho}{\partial \xi_3}\right] \tag{9}$$

$$= \frac{1}{Re}\left[\frac{1}{g_{22}}\left(\frac{\partial \mu}{\partial \xi_2} \frac{\partial u}{\partial \xi_2} + \mu \frac{\partial^2 u}{\partial \xi_2^2}\right) - \frac{g_{22} g_{13}}{g}\left(\frac{\partial \mu}{\partial \xi_2} \frac{\partial v}{\partial \xi_3}\right.\right.$$

$$+ \frac{1}{3} \mu \frac{\partial^2 v}{\partial \xi_2 \partial \xi_3} - \frac{2}{3} \frac{\partial \mu}{\partial \xi_3} \frac{\partial v}{\partial \xi_2}\Big) - \frac{1}{3} \frac{g_{22} g_{13}}{g}\left(\frac{\partial \mu}{\partial \xi_3} \frac{\partial w}{\partial \xi_3} + \mu \frac{\partial^2 w}{\partial \xi_3^2}\right)$$

$$\left. + \frac{g_{11} g_{22}}{g}\left(\frac{\partial \mu}{\partial \xi_3} \frac{\partial u}{\partial \xi_3} + \mu \frac{\partial^2 u}{\partial \xi_3^2}\right)\right]$$

where the velocity vector is written as

$$V = u\, \underline{g}_1 + v\, \underline{g}_2 + w\, \underline{g}_3 \quad . \tag{10}$$

The boundary conditions at the body are the no-slip conditions, a specified enthalpy and the pressure solved by using the v-momentum equation. The Rankine-Hugoniot jump conditions are used at the shock.

The equations are solved by implicit differencing in the ξ_2-ξ_3 plane. The resulting algebraic equations are solved by the Newton-Raphson/Gauss Seidel iteration presented in References 1 and 2. A plane of initial condition data downstream of the sonic plane is required in order to obtain a solution. This is obtained in the present case by utilizing an asixsymmetric shock layer solution for the spherical nose region and transforming this solution into the coordinate system of the PNS equations at the sphere-cone juncture.

3. CONCLUSIONS AND RESULTS

The heat transfer, force and moment coefficients and surface pressure results of four computed cases (Table 1) have been compared against wind tunnel data obtained by Arnold Engineering and Development Center (AEDC). Selected results for the 14/7 biconic with cuts and slice at 10° angle of attack (Case 4) are presented here. Figure 4 describes the body geometry used. The body has a plane of symmetry and a nose radius of 1/2 inch. Figure 5 compares the measured and calculated force and moment coefficients for a similar body but with only a windward cut. Excellent agreement between the predictions and the measurements are obtained.

The remainder of the comparisons will be surface pressure and heat transfer results and will be for the exact geomety of Figure 4. Figure 6 compares the heat transfer over the biconic and cut regions. The axial distance is measured in nose radii

from the apex of the 14^{o} cone. On the windward side and at 90 degrees the agreement is very good. On the leeward side up to just past the biconic junction the agreement is also very good, but then the solution starts to diverge from the data. It is felt that this is due to transition from laminar to turbulent flow. For the $\alpha=10^{o}$ case, separation in the circumferential direction first occurs on the 14^{o} fore-cone near the leeside, but presents no running problems for the code.

Figure 7 is a comparison of the wall pressure from the HYTAC calculations and the AEDC data and also an inviscid calculation[11]. The windward side pressures agree quite well, and on the leeward side the data and HYTAC results are also in agreement. The axial distance in this plot is in inches from the tip of the blunt body. Figures 8 and 9 are circumferential plots of the wall pressure and heat transfer comparing the HYTAC results with the data in the cut region at an axial distance of Z = 21.77" (from the blunt nose). In these plots the X-axis is in inches from the plane of symmetry of the body.

The new non-orthogonal body-normal shock-normal coordinate system works extremely well. Only 25 points in the normal direction are needed to obtain good resolution. With 19 circumferential points the solution over an entire body is obtained with 90 axial steps in approximately 5 minutes on a CDC 7600. The fast running time and good agreement with data is felt to be due in large part to the new coordinate system.

REFERENCES

1. Lubard, S.C. and W.S. Helliwell, "Calculation of the Flow on a Cone at High Angle Attack", AIAA Journal, Vol. 12, No. 7, July 1974, pp. 965-974.

2. Helliwell, W.S. and S.C. Lubard, "An Implicit Method for Three-Dimensional Viscous Flow with Application to Cones at Angle of Attack", Journal of Computers and Fluids, Vol. 3, 1975, pp. 83-101.

3. Adams, J.C., "Numerical Calculation of the Three-Dimensional Hypersonic Viscous Shock Layer on a Sharp Cone at Incidence", Proceedings 1976 Heat Transfer and Fluid Mechanics Institute.

4. Lubard, S.C. and J.V. Rakich, "Calculations of the Flow on a Blunted Cone at High Angle of Attack", AIAA Paper 75-149, 13th Aerospace Science Meeting, Pasadena, Calif., January 1975.

5. Waskiewiez, J.D. and C.H. Lewis, "Hypersonic Viscous Flows over Sphere Cones at High Angle of Attack", AIAA 16th Aerospace Science Meeting, January 1978.

5. Agarwal, R. and J.V. Rakich, "Computation of Hypersonic Viscous Flow Past Spinning Sharp and Blunt Cones at High Angle of Attack", AIAA 16th Aerospace Sciences Meeting, January 1978.

7. Mayne, A.W., Jr., "Calculation of the Laminar Viscous Shock Layer on a Blunt Biconic Body at Incidence to Supersonic and Hypersonic Flow", AIAA Paper 77-88, 15th Aerospace Sciences Meeting, Los Angeles, Calif., 1977.

8. Vigneron, Y.C., J.V. Rakich, and J.C. Tannehill, "Calculations of Supersonic Flow over Delta Wings with Sharp Subsonic Flow over Delta Wings with Sharp Leading Edges", AIAA Paper 78-1137, 11th Fluid and Plasma Dynamics Conference, July 1978.

9. Agopian, K.G., J. Collins, W. Helliwell, S.C. Lubard, and J. Swan, "NASA Viscous 3-D Flowfield Computations", R&D Associates Technical Report, RDA-TR-5100-007, Octobe- 1975.

10. Blottner, F.G. and M. Ellis, "Three-Dimensional, Incompressible Boundary Layer on Blunt Bodies", Sandia Laboratories, SLA-73-0366, April 1973.

11. Marconi, F., L. Yaeger, and M. Salas, "Development of a Computer Code for Calculating the Steady Super-Hypersonic Inviscid Flow Around Real Configurations", Volumes I and II, Computational Techniques, NASA, CR-2675 and CR-2676.

Table 1. Computed and Experimental Cases.

RUN	MACH NO.	$Re_\infty/ft.$	BICONIC	T_0(°R)	CUT BODY	T_w(°R)	ANGLE OF ATTACK
1	10.1	1.8×10^6	9.3/5	1900	NO	1292	2°
2	10	1×10^6	14/7	1900	YES	560	0°
3	10	1×10^6	14/7	1900	YES	560	2°
4	10	1×10^6	14/7	1900	YES	560	10°

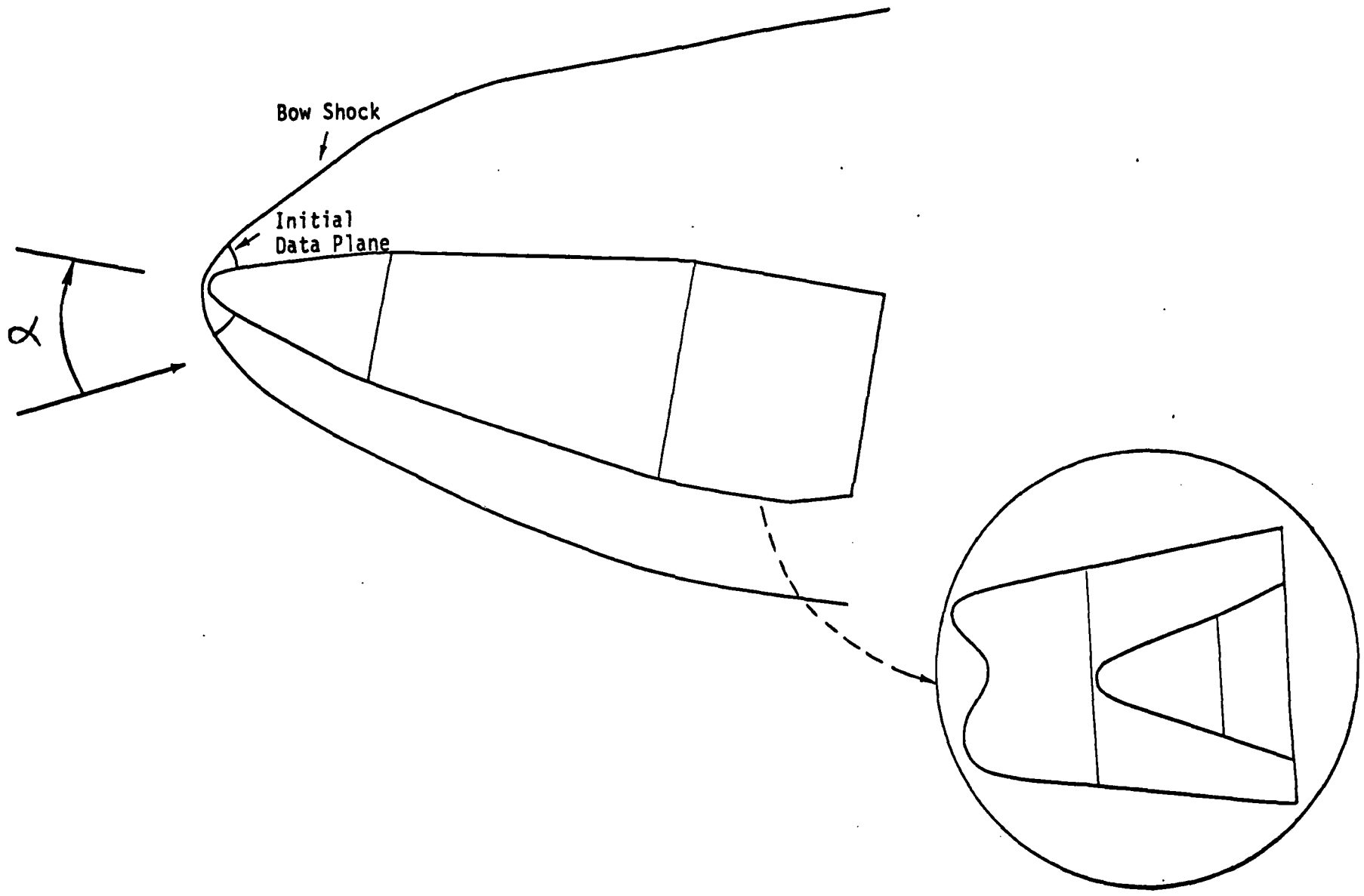

Figure 1. Typical Geometry at Angle of Attack

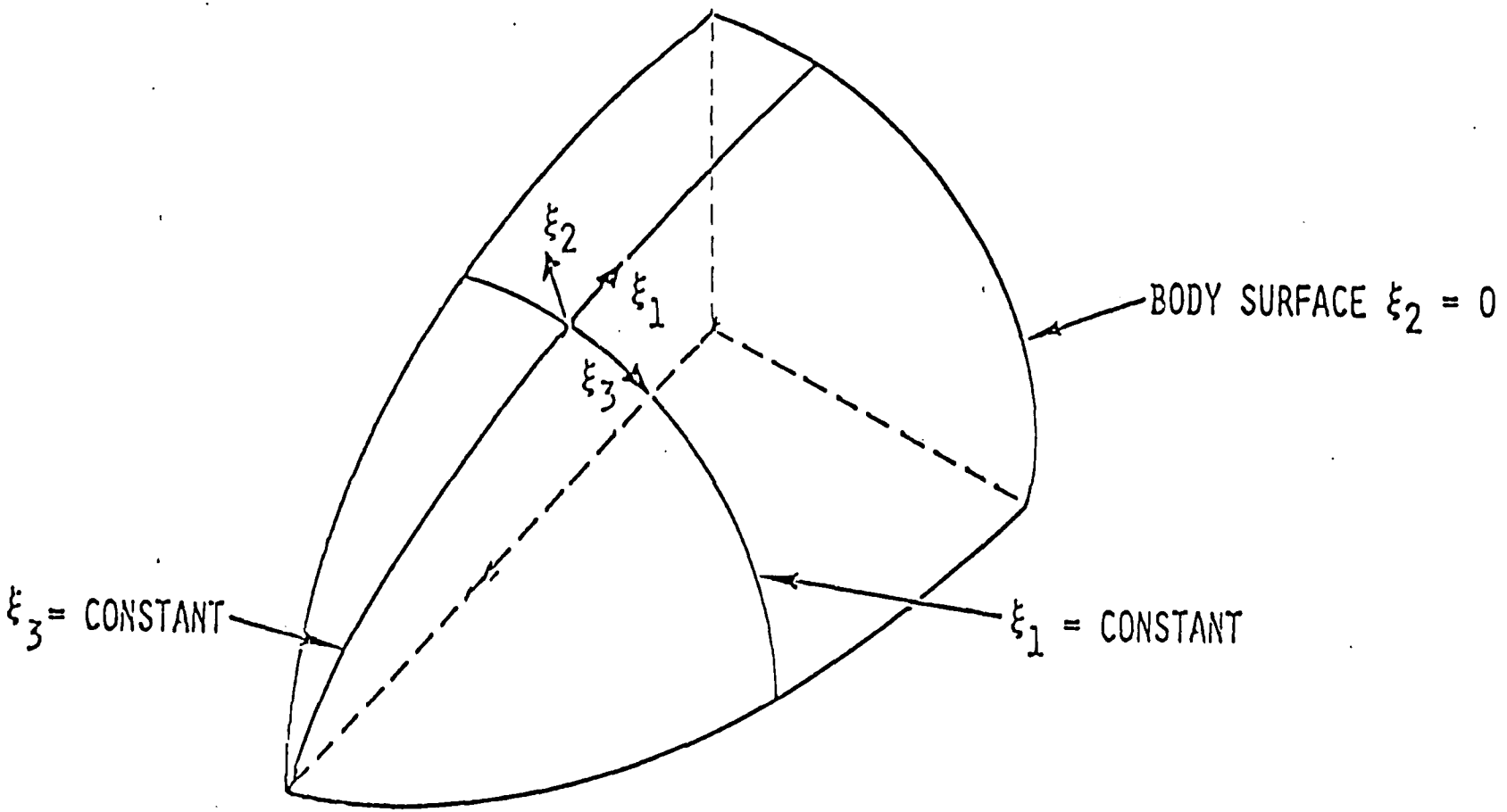

Figure 2. Coordinate System Local to Body

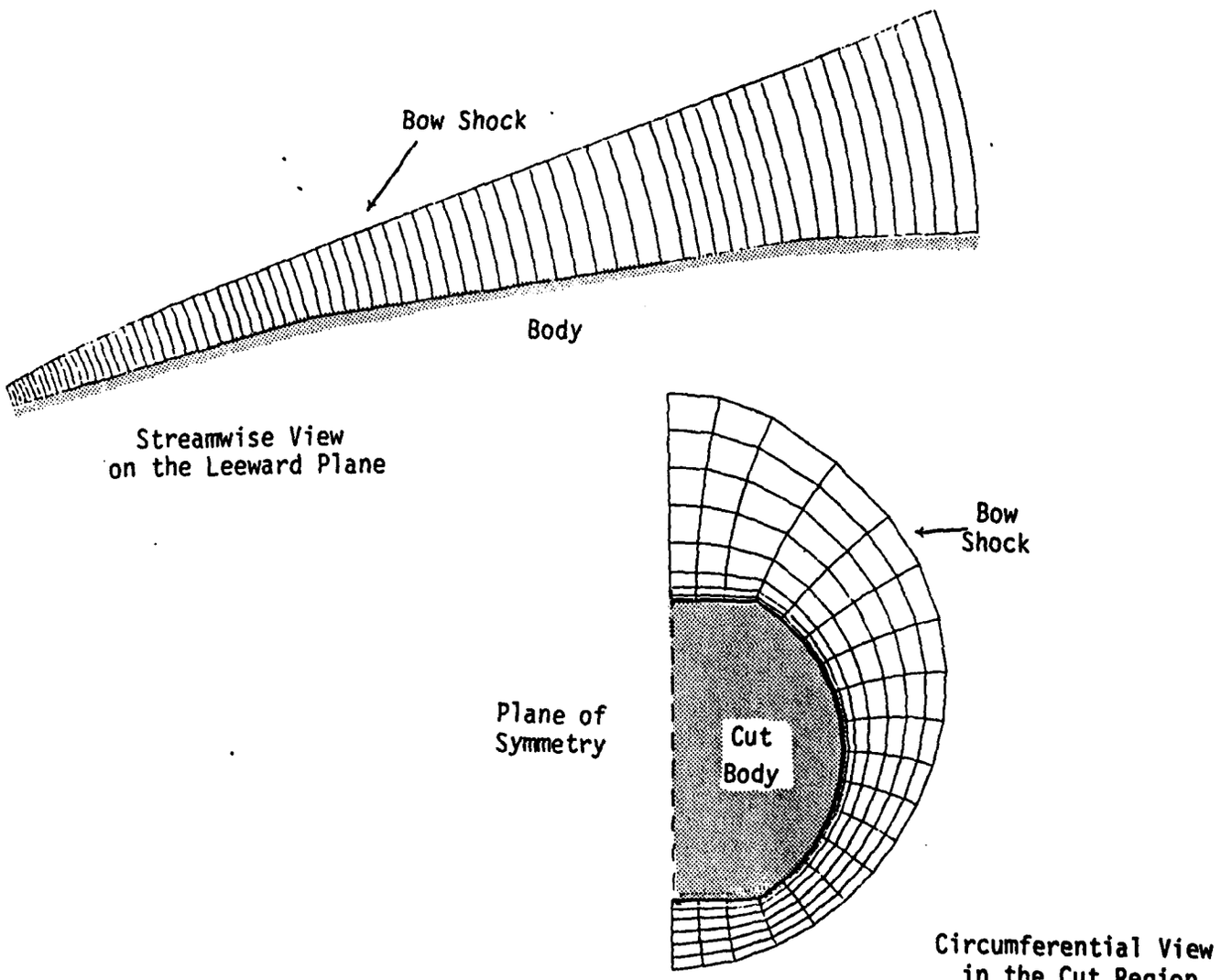

Figure 3. Body Normal - Shock Normal Coordinates

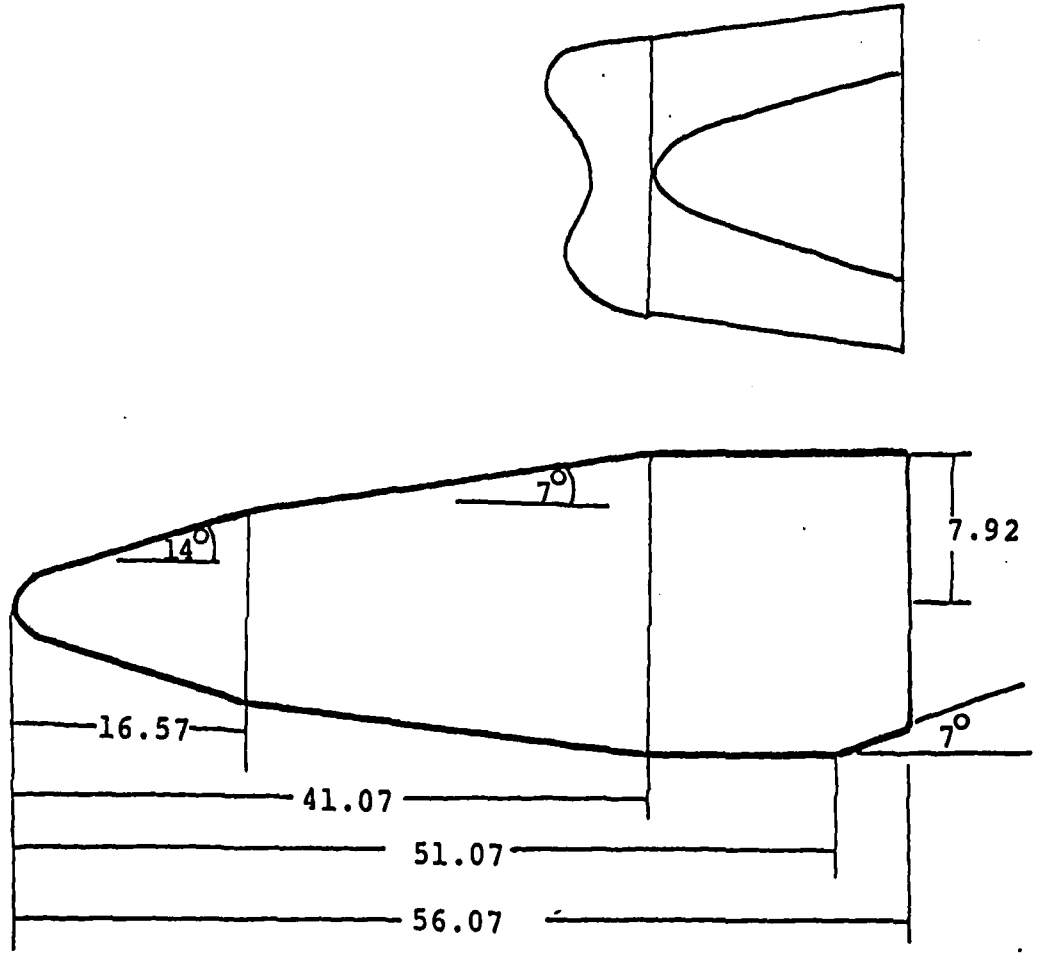

DIMENSIONS IN NOSE RADII (1/2 INCH)

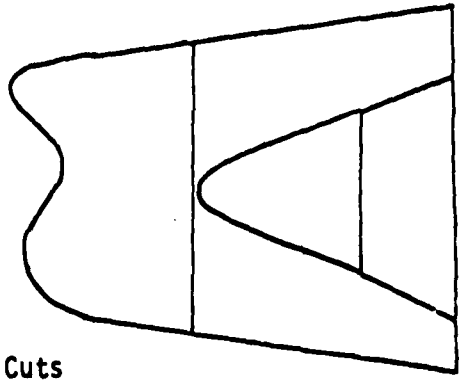

Figure 4. 14/7 Biconic with Cuts

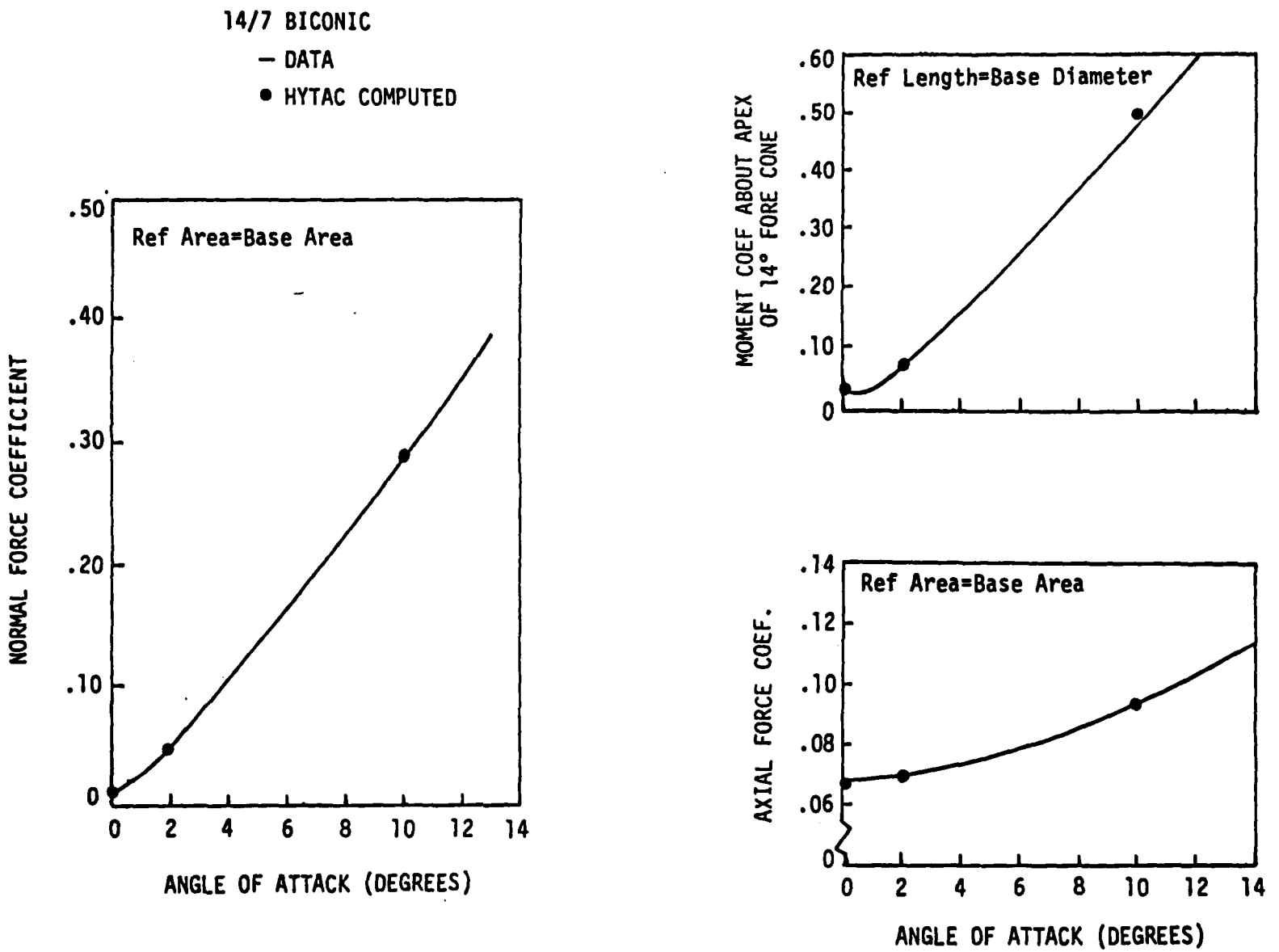

Figure 5. Force and Moment Coefficient Comparisons for a 14/7 Biconic with Windward Cut

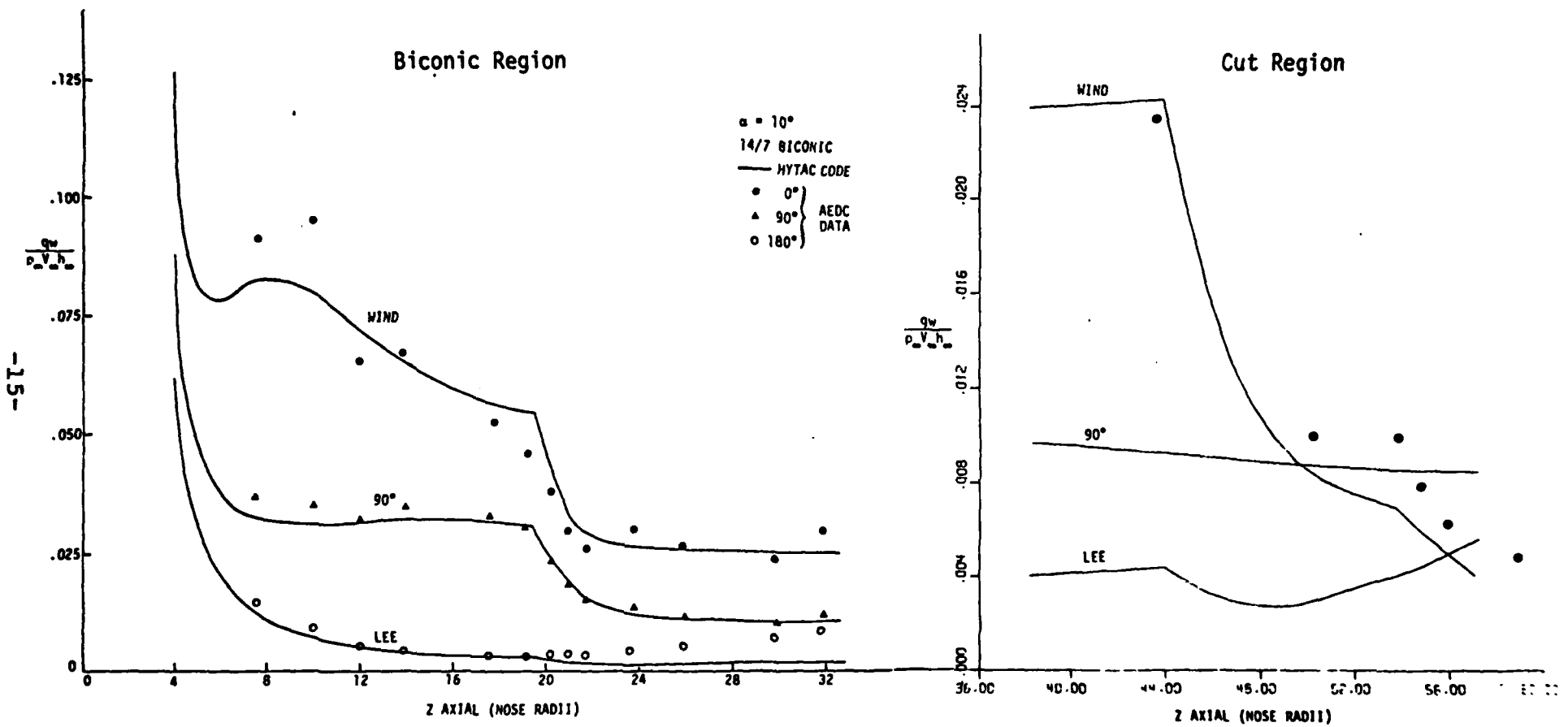

Figure 6. Heat Transfer Results

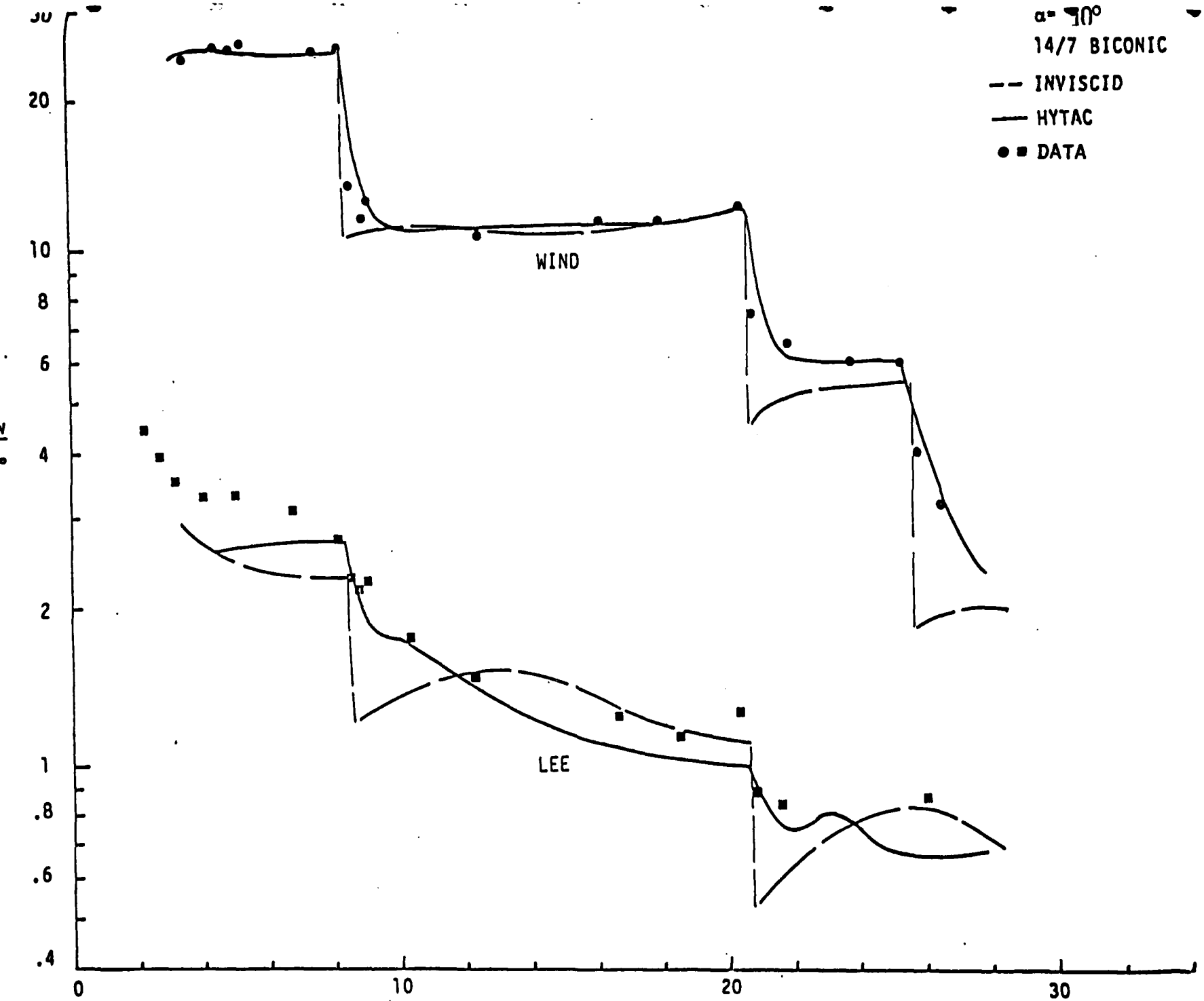
α= 10°
14/7 BICONIC
INVISCID
HYTAC
DATA
WIND
LEE
$\frac{P_W}{P_\infty}$
30
20
10
8
6
4
2
1
.8
.6
.4
0
10
20
30
Z (AXIAL INCHES FROM NOSE)

Figure 7.

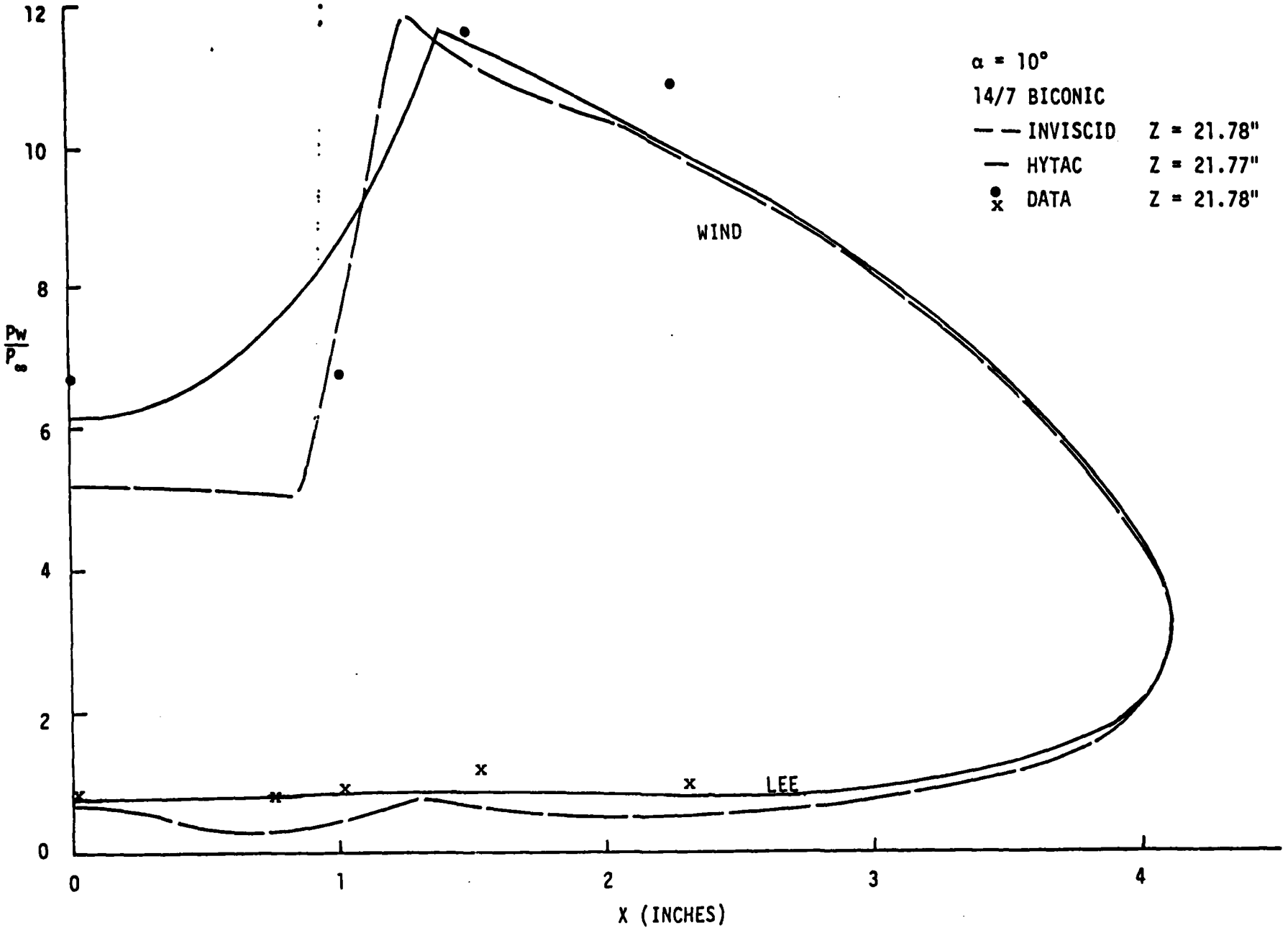

Figure 8. Surface Pressure Results Cut Region (Z = 21.77"), α = 10°

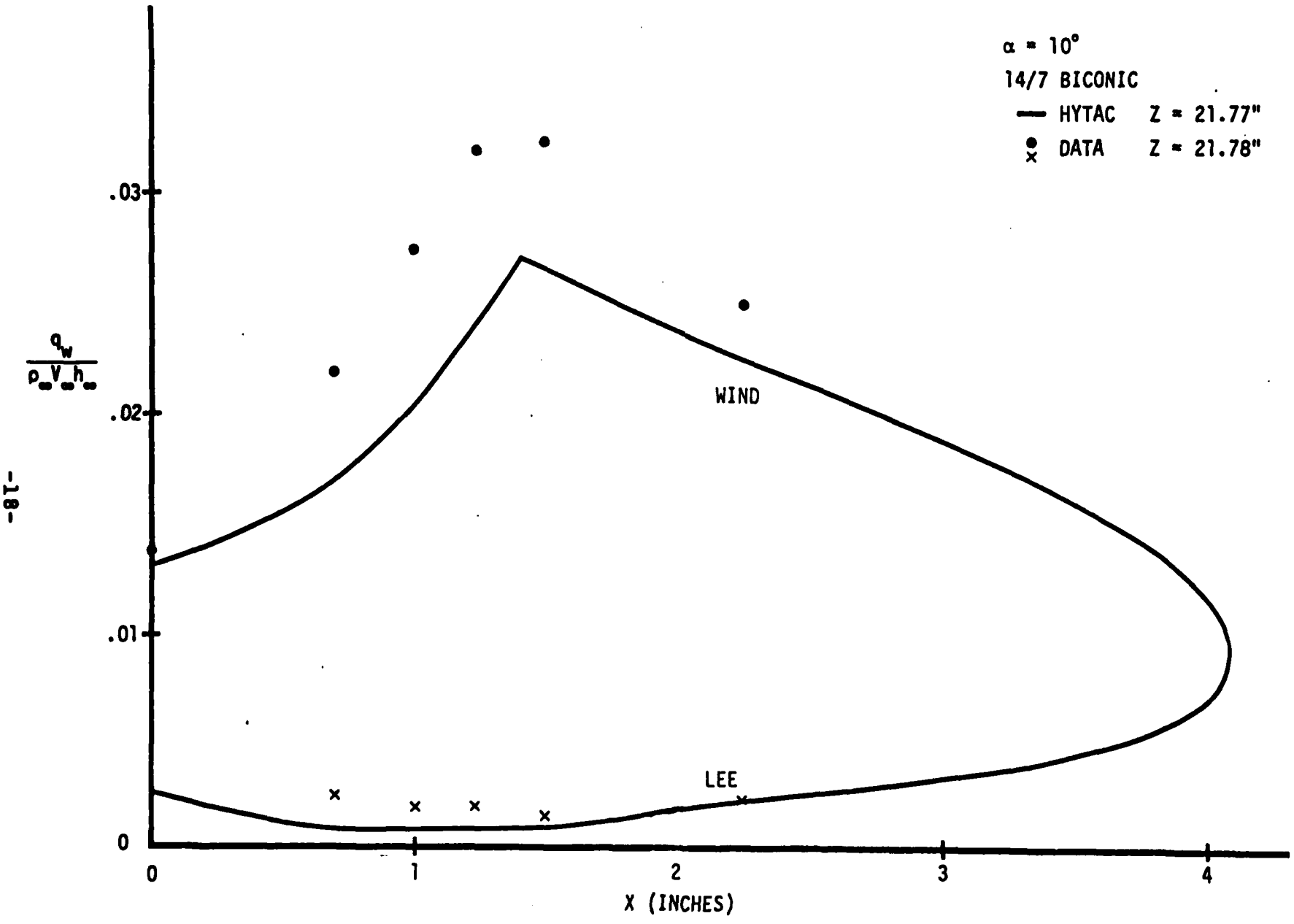

Figure 9. Heat Transfer Results Cut Region (Z = 21.77"), α = 10°